Chaos, Solitons and Fractals 133 (2020) 109636

Contents lists available at ScienceDirect

Chaos, Solitons and Fractals

Nonlinear Science, and Nonequilibrium and Complex Phenomena

journal homepage: www.elsevier.com/locate/chaos

Soliton generation in optical fiber networks

K.K. Sabirov[a,b], M.E. Akramov[c,*], R. Sh. Otajonov[d], D.U. Matrasulov[a,e]

[a] Turin Polytechnic University in Tashkent, 17 Niyazov Str., Tashkent 100095, Uzbekistan
[b] Tashkent University of Information Technologies, 108 Amir Temur Str., Tashkent 100200, Uzbekistan
[c] National University of Uzbekistan, Vuzgorodok, Tashkent 100174, Uzbekistan
[d] Physical-Technical Institute, Uzbekistan Academy of Sciences, 2-b, Bodomzor str., Tashkent 100084, Uzbekistan
[e] Center for Nanotechnologies, National University of Uzbekistan, Vuzgorodok, Tashkent 100174, Uzbekistan

ARTICLE INFO

Article history:
Received 24 October 2019
Revised 5 January 2020
Accepted 15 January 2020

Keywords:
optical fiber network
optical solitons
pulse generation
soliton transport

ABSTRACT

We consider the problem of soliton generation in branched optical fibers. A model based on the nonlinear Schrodinger equation on metric graphs is proposed. Number of generated solitons is computed for different branching topologies considering different initial pulse profiles. Experimental realization of the model is discussed.

© 2020 Elsevier Ltd. All rights reserved.

1. Introduction

Optical solitons attracted much attention due to their potential applications in optoelectronics and information technologies. The idea of using optical solitons as carriers of information in high-speed communication systems was first proposed in the pioneering paper by Hasegawa and Tappert [1]. Later due to the advances made in fiber technology it became possible to realize optical solitons experimentally in different versions (bright, dark, etc) [2–11]. This fact caused great interest to finding the soliton solutions of governing nonlinear wave equations, such as nonlinear Schödinger equations with different nonlinearities. An important problem in the context of optical solitons is the problem of soliton generation in optical media. Mathematically, such problem is reduced to the initial value (Cauchy) problem for nonlinear Schödinger equation, which allows to find soliton solution and number of generated solitons using given initial condition. For optical fibers such problem was studied in the Refs. [12–25]. In [12] an effective method for finding number of solitons generated in optical fibers was proposed. Later, it was extended for some other initial conditions [13]. Strict mathematical treatment of soliton generation on a half line as initial-boundary-value problem was considered presented [15]. Soliton generation in optical fibers for a dual-frequency input was studied in [16]. In [19] a theory of the generation of new spectral components in optical fibers pumped with a solitonic pulse and a weak continuous wave was proposed and the wave number matching conditions for this process was derived. In [17] characteristics of wavelength-tunable femtosecond soliton pulse generation using optical fibers in a negative dispersion region are studied experimentally and theoretically using the extended nonlinear Schrödinger equation, in which the wavelength dependence of parameters is considered. A comprehensive analysis of the generation of optical solitons in a monomode optical fibre from a superposition of soliton-like optical pulses at different frequencies in [18], where it is found that there exists a critical frequency separation above which wavelength-division multiplexing with solitons is feasible. Soliton generation and their instability are investigated in a system of two parallel-coupled fibers, with a pumped (active) nonlinear dispersive core and a lossy (passive) linear one in [20]. A theory of the generation of new spectral components in optical fibers pumped with a solitonic pulse have been studied. Bright-gap-soliton generation in finite optical lattices was discussed in [21]. Despite the fact that certain progress is made on theoretical and experimental study of soliton generation in optical fibers, all the studies are restricted by considering long, unbranched fibers. However, branched fibers are more attractive from the viewpoint of practical applications, as in may cases information-communication systems use optical fiber networks. Modeling of soliton generation and dynamics in optical fiber networks requires solving of nonlinear Schödinger equation on metric graphs.

We note that soliton dynamics described by integrable nonlinear wave equations attracted much attention during past decade

* Corresponding author.
E-mail address: akramov.mashrabboy@mail.ru (M.E. Akramov).

https://doi.org/10.1016/j.chaos.2020.109636
0960-0779/© 2020 Elsevier Ltd. All rights reserved.

[26–38]. In [26] nonlinear Schödinger equation on metric graphs is studied and condition for integrability is derived in the form of a sum rule for nonlinearity coefficients. In [27] such study is extended to Ablowitz-Laddik equation. Stationary Schödinger equation on metric graphs and standing wave soliton in networks are studied in [28–30,34,36]. Integrable sine-Gordon equation on metric graphs is studied in [31,35,38]. Linear and nonlinear systems of PDE on metric graphs are considered in [39–41].

In this paper we consider the problem of soliton generation in branched optical fibers, or optical fiber networks described in terms of the initial value problem for nonlinear Schödinger equation on metric graphs. For different given initial conditions, we derive number of solitons generated by considering different network topologies. Unlike linear optical fibers, pulse generation and soliton dynamics in fiber networks strongly depend on the topology of latter. Propagating in such network optical soliton undergo to scattering and transmission through the network branching points that may cause additional effects such as interaction of incoming and scattered solitons, radiation, collisions, etc. Therefore effective transmission of information through the optical fiber networks requires proper tuning both the system architecture and initial pulse profiles. Depending on which branch, or vertex the initial pulse located, the number of solitons and their dynamics can be different. This fact provides powerful tool for tuning of the optical fiber network architecture and optimization of signal and information transmission.

This paper is organized as follows. In the next section we briefly recall treatment of the problem of soliton generation for linear (unbrached) optical fibers. In Section 3 we give formulation of the problem and its solution for star branched (Y-junction) optical fibers. Section 4 extends the study for other network topologies, modeled by H- and tree graphs. Section 5 presents some concluding remarks.

2. Soliton generation in linear optical fibers

Let us first, following the Refs. [12,13], recall solution of the problem for linear, i.e. unbranched optical fibers. The governing equation for the pulse generation and evolution in optical fibers is the following nonlinear Schödinger equation

$$i\frac{\partial\psi}{\partial t}+\frac{1}{2}\frac{\partial^2\psi}{\partial x^2}+|\psi|^2\psi=0, \tag{1}$$

where ψ is the normalized complex amplitude of the pulse envelope. The problem of soliton generation in optical fibers is reduced to the Cauchy problem for Eq. (1). Such problem can be solved, e.g., using inverse scattering method [12,13,16]. In [12] it was solved for the initial conditions given by $\psi(x,0)=-iq(x)$, with

$$q(x)=\begin{cases}0, & \text{for} \quad |x|>\frac{1}{2}a\\ b, & \text{for} \quad |x|\le\frac{1}{2}a\end{cases} \qquad b>0. \tag{2}$$

The evolution of the wave function upon generation of the soliton can be obtained via solving the following eigenvalue problem

$$Au=\lambda u, \tag{3}$$

where

$$A=\begin{pmatrix} i\frac{d}{dx} & \psi(x,0)\\ -\psi^*(x,0) & -i\frac{d}{dx}\end{pmatrix}. \tag{4}$$

Each discrete eigenvalue $\lambda=\xi+i\eta$ with L^2- integrable eigenfunction corresponds to the generated soliton with the amplitude 2η moving with the velocity 2ξ.

It was shown in [12] that number of generated solitons is given by expression

$$N=\left\langle\frac{1}{2}+\frac{F}{\pi}\right\rangle, \tag{5}$$

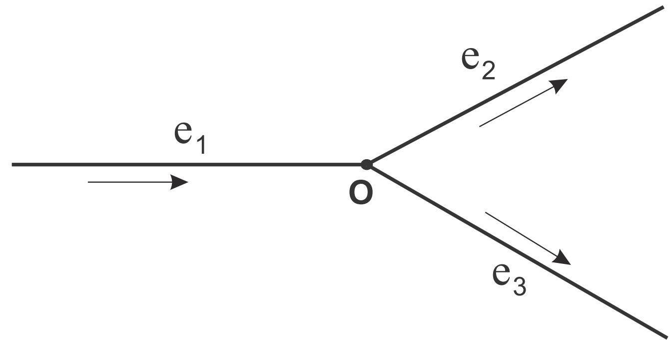

Fig. 1. Basic star graph.

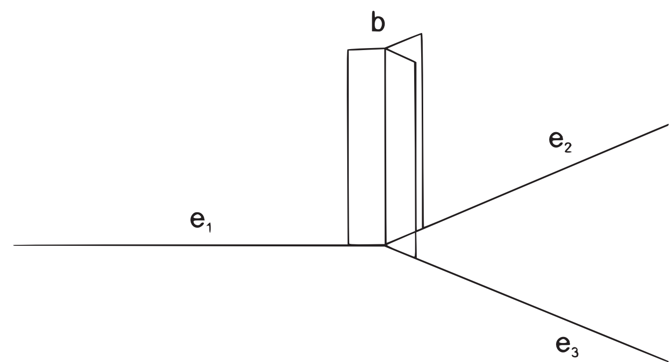

Fig. 2. Initial pulse profile in the star branched optical fiber.

where $F=\int_{-\infty}^{\infty}|\psi(x,0)|dx$ and $<\ldots>$ denotes the integer smaller than the argument. Similar result for the number of solitons was obtained in the Ref. [12] for the initial condition given by

$$q(x)=\beta\exp(-\alpha|x|),\quad \alpha,\beta>0.$$

Later, Kivshar considered the problem of soliton generation for super Gaussian initial pulse and showed that Eq. (5) is general formula for arbitrary initial profile [13]. More detailed treatment of the problem of soliton generation in optical fibers was presented in [16]. In particular, the authors of [16] analyzed scenarios for soliton generation in an ideal fiber for an input that consists of either two in-phase or out-of-phase solitonlike optical pulses at different frequencies by considering symmetric and asymmetric initial input pulses. In the next section we extend these studies to the case of branched optical fibers, i.e. fiber networks.

3. Description of the model for star shaped network

Soliton dynamics in networks has attracted much attention during past decade. Convenient approach to describe such system is modeling in terms of nonlinear wave equation on a metric graph. The early treatment of the nonlinear Schrodinger equation on metric graphs dates back to the Ref. [26], where soliton solutions of the NLSE on metric graphs was obtained and integrability of the problem under certain constraints was shown by proving the existence of an infinite number of conserving quantities, (Fig. 2).

Here we briefly recall the problem of NLSE in metric star graph following the Ref. [26]. Consider the star graph with three bonds e_j (see, Fig. 1), for which a coordinate x_j is assigned. Choosing the origin of coordinates at the vertex, 0 for bond e_1 we put $x_1\in(-\infty,0]$ and for $e_{2,3}$ we fix $x_{2,3}\in[0,+\infty)$. In what follows, we use the shorthand notation $\Psi_j(x)$ for $\Psi_j(x_j)$ where x is the coordinate on the bond j to which the component Ψ_j refers. The nonlinear Schrödinger equation on each bond e_j of such graph can be written as [26]

$$i\frac{\partial \psi_j}{\partial t} + \frac{\partial^2 \psi_j}{\partial x^2} + \beta_j |\psi_j|^2 \psi_j = 0, \tag{6}$$

where the nonlinearity parameter, β_j is determined in terms of the nonlinear refractive index of the material for each branch of the network [10]. To solve Eq. (6) one needs to impose the boundary conditions at the branching point. This can be derived from the fundamental physical laws, such as norm and energy conservation, which are given as [26]

$$\frac{dN}{dt} = 0, \quad \frac{dE}{dt} = 0, \tag{7}$$

where

$$N(t) = \int_{-\infty}^{0} |\psi_1|^2 dx + \int_0^{\infty} |\psi_2|^2 dx + \int_0^{\infty} |\psi_3|^2 dx$$

and

$$E = E_1 + E_2 + E_3,$$

with

$$E_k = \int_{e_k} \left[\left| \frac{\partial \psi_k}{\partial x} \right|^2 - \frac{\beta_k}{2} |\psi_k|^4 \right] dx.$$

As it was shown in the Ref. [26], the conservation laws Eq. (7) lead to the following vertex conditions

$$\sqrt{\beta_1}\psi_1(0,t) = \sqrt{\beta_2}\psi_2(0,t) = \sqrt{\beta_3}\psi_3(0,t), \tag{8}$$

and generalized Kirchhoff rules

$$\frac{1}{\sqrt{\beta_1}} \frac{d\psi_1}{dx}|_{x=0} = \frac{1}{\sqrt{\beta_2}} \frac{d\psi_2}{dx}|_{x=0} + \frac{1}{\sqrt{\beta_3}} \frac{d\psi_3}{dx}|_{x=0}, \tag{9}$$

where β_j are nonzero real constants. The asymptotic conditions for Eq. (1) are imposed as

$$\lim_{|x|\to+\infty} \psi_j = 0. \tag{10}$$

The single soliton solutions of Eq. (1) fulfilling the vertex boundary conditions (8), (9) and the asymptotic condition, (10) can be written as [26]

$$\psi_j(x,t) = a\sqrt{\frac{2}{\beta_j}} \frac{\exp\left[i\frac{vx}{2} - i(\frac{v^2}{4} - a^2)t\right]}{\cosh[a(x - l - vt)]}, \tag{11}$$

where the parameters β_j fulfill the sum rule [26]

$$\frac{1}{\beta_1} = \frac{1}{\beta_2} + \frac{1}{\beta_3}. \tag{12}$$

Here v, l and a are bond-independent parameters characterizing velocity, initial center of mass and amplitude of a soliton, respectively. In experiment, sum rule in Eq. (12) can be fulfilled by proper tuning of refractive index for each branch of the optical fiber network.

Consider branched optical fiber having the form of the Y-junction. Such system can be considered as basic star graph presented in Fig. 1. Then the problem of generation of soliton and its propagation can be modeled in terms of the Cauchy problem for nonlinear Schödinger equation on a basic star graph, which is given by Eq. (6) for which the following initial condition is imposed:

$$\psi_j(x,0) = -i\sqrt{\frac{2}{\beta_j}} q_j(x).$$

Here ψ_j is the normalized complex amplitude of the pulse envelope on jth bond (branch) of the graph and $q_j(x)$ is the initial profile of the amplitude. To solve this equation, one needs to impose the boundary conditions at the branching point (vertex) of the graph and determine the asymptotic of the wave function at the branch ends. These can be written in the form of Eqs. (8), (9) and (10).

Here we consider the problem of soliton generation for Y-junction of the optical fiber for the initial pulse profile given as (see, Fig. 2)

$$q_1(x) = \begin{cases} 0, & x < -\frac{1}{2}a \\ b, & -\frac{1}{2}a \le x \le 0 \end{cases} \tag{13}$$

$$q_{2,3} = \begin{cases} 0, & x > \frac{1}{2}a \\ b, & 0 \le x \le \frac{1}{2}a \end{cases} \tag{14}$$

Such initial profile implies that soliton is generated around the branching point on each branch. Using the inverse scattering based approach (see, Appendix A), one can compute the number of generated solitons, N for such profile:

$$N = \left\langle \frac{3}{2} + \frac{F}{\pi} \right\rangle, \tag{15}$$

where

$$F = \sum_{j=1}^{3} \int_{e_j} |\psi_j(x,0)| dx = \frac{ab}{2}\left[\sqrt{\frac{2}{\beta_1}} + \sqrt{\frac{2}{\beta_2}} + \sqrt{\frac{2}{\beta_3}}\right]. \tag{16}$$

We assume that the sum rule is (12) is fulfilled, i.e. the problem is integrable. Difference between Eqs. (5) and (15) comes from the constant factor

$$(\sqrt{2\beta_1^{-1}} + \sqrt{2\beta_2^{-1}} + \sqrt{2\beta_3^{-1}}).$$

This allows tuning the soliton number and dynamics using different choices of the set β_j, $(j = 1, 2, 3)$. In addition, for simplicity, the above initial pulse profiles in Eqs. (13) and (14) are given at the vertex and have the same widths, a and heights, b. However, in general case one can choose different widths and heights for different bonds. This also provides additional tool for tuning of the soliton number and dynamics.

Another initial pulse profile, for which the soliton number and solutions in a Y-junction fiber can be explicitly obtained is given by

$$\psi_j(x,0) = \sqrt{\frac{2}{\beta_j}} \mathrm{sech}(x)\left[e^{i(\omega x + \frac{\theta}{2})} + e^{-i(\omega x + \frac{\theta}{2})}\right], \tag{17}$$

where 2ω and θ are the frequency detuning and the phase difference between the two solitons, correspondingly. The two-soliton solution of the problem given by Eqs. (6), (8) and (9) can be written as

$$\psi_j(x,t) = \sqrt{\frac{2}{\beta_j}} \xi\eta e^{\phi(\frac{t}{2})} \times \frac{e^{i\xi x}\cosh[\eta(x+\xi t) + i\varphi] + e^{-i\xi x}\cosh[\eta(x-\xi t) - i\varphi]}{\xi^2\cosh\eta(x+\xi t)\cosh\eta(x-\xi t) + \eta^2\sin\xi(x+i\eta t)\sin\xi(x-i\eta t)}, \tag{18}$$

which is valid under the constraint:

$$\frac{1}{\beta_1} = \frac{1}{\beta_2} + \frac{1}{\beta_3}, \tag{19}$$

Corresponding soliton number is given by Eq. (15), where the quantity F can be written as

$$F = 2\pi\left(\sqrt{\frac{2}{\beta_1}} + \sqrt{\frac{2}{\beta_2}} + \sqrt{\frac{2}{\beta_3}}\right)\mathrm{sech}\left(\frac{\pi\omega}{2}\right)\cos\left(\frac{\theta}{2}\right)$$

Finally, the pulse profile, which is more realistic and is often used in experiments is Gaussian profile, which is given by

$$\psi_j(x,0) = \sqrt{\frac{2}{\beta_j}} A\exp\left[-\frac{1}{2}(1-i\alpha)\left(\frac{x}{\sigma}\right)^{2m}\right] \tag{20}$$

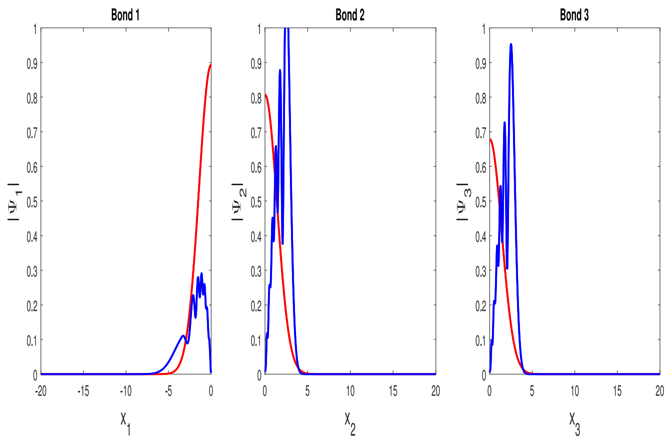

Fig. 3. Profile of the wave function, $|\psi(x,t)|$ at $t=0$ (red) and $t=0.075$ (blue) on star graph.

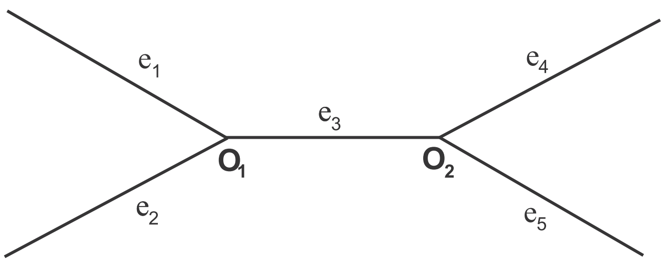

Fig. 4. Sketch for the H-graph.

Using the above approach for this profile leads to

$$F=\sum_{j=1}^{3}\int_{e_j}|\psi_j(x,0)|dx$$
$$=\frac{2^{\frac{1}{2m}}A\sigma}{2m}\Gamma\left(\frac{1}{2m}\right)\left[\sqrt{\frac{2}{\beta_1}}+\sqrt{\frac{2}{\beta_2}}+\sqrt{\frac{2}{\beta_3}}\right],\quad N=\left\langle\frac{3}{2}+\frac{F}{\pi}\right\rangle. \tag{21}$$

Important characteristics of soliton generation is radiation that leads to change in the soliton profile. Here we consider radiation at the vertex by analyzing plots of $|\psi(x,t)|$. Fig. 3 compares profiles of $|\psi(x,t)|$ at $t=0$ and $t=0.075$ for Gaussian initial profile. Breaking of initial profile can be clearly seen.

Finally, we note that the above results are obtained by assuming that the sum rule in Eq. (12) is fulfilled. As it follows from the Ref. [26], no reflection of solitons at the vertex is possible for this case, i.e. transmission of solitons through the vertex is reflectionless. Therefore generation of reflected pulses is not possible for this case, (Figs. 5 and 6).

4. Other network topologies

The above treatment of the problem for soliton generation in optical fiber networks can be extended to the case of more complicated topologies. Here we demonstrate this for so-called $H-$graph and tree graph. For H-graph, presented in Fig. 4 the coordinates are defined as $x_{1,2}\in(-\infty;0]$, $x_3\in[0;L]$, $x_{4,5}\in[0;+\infty)$, where L is the length of bond e_3, i.e. the distance between two vertices.

For NLS Eq. (6) and the vertex boundary conditions given by

$$\sqrt{\beta_1}\psi_1(0,t)=\sqrt{\beta_2}\psi_2(0,t)=\sqrt{\beta_3}\psi_3(0,t),$$
$$\sqrt{\beta_3}\psi_3(L,t)=\sqrt{\beta_4}\psi_4(0,t)=\sqrt{\beta_5}\psi_5(0,t), \tag{22}$$

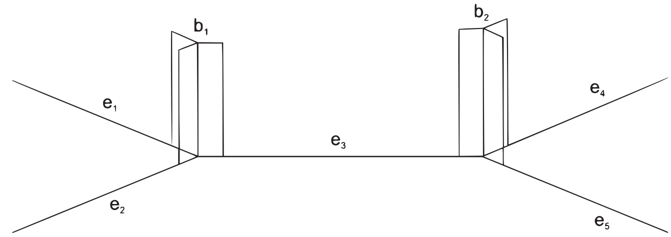

Fig. 5. Initial pulse profile on the optical fiber H-shaped network.

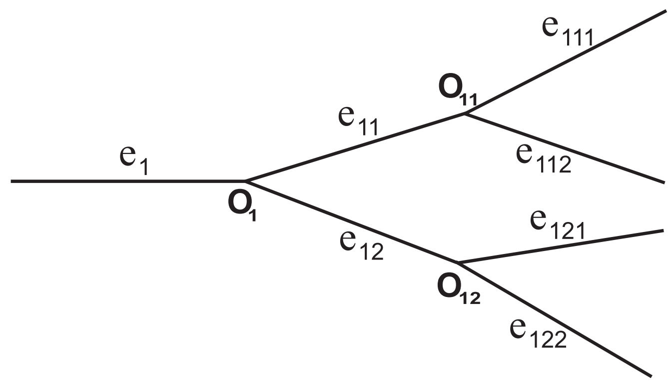

Fig. 6. Sketch for tree graph.

$$\frac{1}{\sqrt{\beta_1}}\frac{d\psi_1}{dx}|_{x=0}+\frac{1}{\sqrt{\beta_2}}\frac{d\psi_2}{dx}|_{x=0}=\frac{1}{\sqrt{\beta_3}}\frac{d\psi_3}{dx}|_{x=0},$$
$$\frac{1}{\sqrt{\beta_3}}\frac{d\psi_3}{dx}|_{x=L}=\frac{1}{\sqrt{\beta_4}}\frac{d\psi_4}{dx}|_{x=0}+\frac{1}{\sqrt{\beta_5}}\frac{d\psi_5}{dx}|_{x=0}. \tag{23}$$

We consider the following initial conditions:

$$\psi_j(x,0)=-i\sqrt{\frac{2}{\beta_j}}q_j(x)$$

where the initial pulse profiles are given by (see, Fig. 5)

$$q_{1,2}(x)=\begin{cases}0, & -\infty<x<-\frac{1}{2}a\\ b_1, & -\frac{1}{2}a\le x\le 0\end{cases} \tag{24}$$

$$q_3(x)=\begin{cases}b_1, & 0\le x\le\frac{1}{2}a\\ 0, & \frac{1}{2}a<x<L-\frac{1}{2}a\\ b_2, & L-\frac{1}{2}a\le x\le L\end{cases} \tag{25}$$

$$q_{4,5}(x)=\begin{cases}b_2, & 0\le x\le\frac{1}{2}a\\ 0, & \frac{1}{2}a<x<\infty\end{cases} \tag{26}$$

Then the number of generated optical solitons in such system we have explicit expression:

$$N=\left\langle\frac{5}{2}+\frac{F_1+F_2}{\pi}\right\rangle, \tag{27}$$

where

$$F_1=\frac{ab_1}{2}\left[\sqrt{\frac{2}{\beta_1}}+\sqrt{\frac{2}{\beta_2}}+\sqrt{\frac{2}{\beta_3}}\right], \tag{28}$$

and

$$F_2=\frac{ab_2}{2}\left[\sqrt{\frac{2}{\beta_3}}+\sqrt{\frac{2}{\beta_4}}+\sqrt{\frac{2}{\beta_5}}\right]. \tag{29}$$

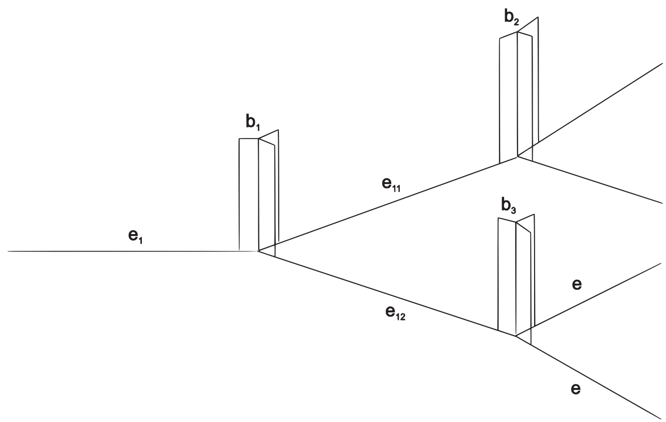

Fig. 7. Initial pulse profile on the tree-shaped optical fiber network.

Similarly, one can find number of generated solitons for the tree graph, presented in Fig. 6. The vertex boundary conditions for such graph are given by

$$\sqrt{\beta_1}\psi_1(0,t) = \sqrt{\beta_2}\psi_2(0,t) = \sqrt{\beta_3}\psi_3(0,t),$$
$$\sqrt{\beta_{1i}}\psi_{1i}(L_{1i},t) = \sqrt{\beta_{1ij}}\psi_{1ij}(0,t),\ i,j=1,2, \tag{30}$$

and

$$\frac{1}{\sqrt{\beta_1}}\frac{d\psi_1}{dx}|_{x=0} = \frac{1}{\sqrt{\beta_2}}\frac{d\psi_2}{dx}|_{x=0} + \frac{1}{\sqrt{\beta_3}}\frac{d\psi_3}{dx}|_{x=0},$$
$$\frac{1}{\sqrt{\beta_{1i}}}\frac{d\psi_{1i}}{dx}|_{x=L_{1i}} = \frac{1}{\sqrt{\beta_{1i1}}}\frac{d\psi_{1i1}}{dx}|_{x=0} + \frac{1}{\sqrt{\beta_{1i2}}}\frac{d\psi_{1i2}}{dx}|_{x=0}. \tag{31}$$

Furthermore, we choose the initial pulse profile at each vertex ($\psi_e(x,0) = -i\sqrt{\frac{2}{\beta_e}}q_e(x)$) in the forms (see, Fig. 7)

$$q_1(x) = \begin{cases} 0, & -\infty < x < -\frac{1}{2}a \\ b_1, & -\frac{1}{2}a \le x \le 0 \end{cases} \tag{32}$$

$$q_{11}(x) = \begin{cases} b_1, & 0 \le x \le \frac{1}{2}a \\ 0, & \frac{1}{2}a < x < L_{11} - \frac{1}{2}a \\ b_2, & L_{11} - \frac{1}{2}a \le x \le L_{11} \end{cases} \tag{33}$$

$$q_{12}(x) = \begin{cases} b_1, & 0 \le x \le \frac{1}{2}a \\ 0, & \frac{1}{2}a < x < L_{12} - \frac{1}{2}a \\ b_3, & L_{12} - \frac{1}{2}a \le x \le L_{12} \end{cases} \tag{34}$$

$$q_{1ij}(x) = \begin{cases} b_{i+1}, & 0 \le x \le \frac{1}{2}a \\ 0, & \frac{1}{2}a < x < \infty \end{cases} \tag{35}$$

where $i, j = 1, 2$, L_{11} and L_{12} are lengths of bonds e_{11} and e_{12} respectively.

Then for the generated soliton number we have

$$N = \left\langle \frac{7}{2} + \frac{F_1 + F_2 + F_3}{\pi} \right\rangle, \tag{36}$$

where

$$F_1 = \frac{ab_1}{2}\left[\sqrt{\frac{2}{\beta_1}} + \sqrt{\frac{2}{\beta_{11}}} + \sqrt{\frac{2}{\beta_{12}}}\right] \tag{37}$$

$$F_2 = \frac{ab_2}{2}\left[\sqrt{\frac{2}{\beta_{11}}} + \sqrt{\frac{2}{\beta_{111}}} + \sqrt{\frac{2}{\beta_{112}}}\right] \tag{38}$$

$$F_3 = \frac{ab_3}{2}\left[\sqrt{\frac{2}{\beta_{12}}} + \sqrt{\frac{2}{\beta_{121}}} + \sqrt{\frac{2}{\beta_{122}}}\right] \tag{39}$$

The number of parameters in Eq. (36) is much higher that in the case of star graph. This implies that tree-shaped optical fiber network provides more wider possibility for tuning the generated soliton number and their dynamics.

5. Conclusions

In this paper we studied the problem of soliton generation in optical fiber networks using a model based NLS equation on metric graphs. Initial value (Cauchy) problem for NLS equation on metric graphs is solved for different graph topologies, such as star, tree and H-graphs. For branched optical fibers one can choose the initial pulse profile in different ways (e.g., at the vertex or branch, at given vertex or branch, with different shapes at different vertices). Therefore, unlike to linear (unbranched) fibers, soliton generation for optical fiber networks have richer dynamics and tools for manipulation by solitons numbers. The above method can be applied for different network topologies, provided a network has three and more semi-infinite outgoing branches. This allows to use our model for the problem of tunable soliton generation in optical fiber networks, which is of importance for practical applications in the areas, where optical fibers are used for information (signal) transfer.

Declaration of Competing Interest

The authors declare that they have no known competing financial interests or personal relationships that could have appeared to influence the work reported in this paper.

Acknowledgements

This work is supported by the grant of the Ministry for Innovation Development of Uzbekistan (Ref. No. BF2-022).

Appendix A

In this appendix, following the Ref. [13], we will provide brief derivation of Eq. (15) describing the relation between the number of generated solitons and the initial pulse profile in star branched optical fibers.

Consider Zakharov–Shabat problem on the star graph:

$$\frac{\partial v_j^{(1)}}{\partial x} = i\lambda v_j^{(1)} + i\psi_j(x,0)v_j^{(2)},$$
$$\frac{\partial v_j^{(2)}}{\partial x} = -i\lambda v_j^{(2)} + i\psi_j^*(x,0)v_j^{(1)}, \tag{40}$$

where $\psi_j(x, 0)$ are the initial conditions (initial pulse profile) for NLS Eq. (6) given on the each bond e_j of the start graph presented in Fig. 1. Let us consider the special family of the initial potentials

$$\psi_j(x,0) = \Psi_j(x,0)e^{i\delta_j}, \tag{41}$$

where $\Psi_j(x, 0)$ are the real functions and $\delta_j (0 \le \delta_j \le 2\pi)$ are arbitrary constants. One can show that the transformations

$$v_j^{(1)} \to V_j^{(1)}e^{i\gamma_j},\ v_j^{(2)} \to V_j^{(2)}e^{i(\gamma_j-\delta_j)} \tag{42}$$

lead to the following eigenvalue problem

$$\frac{\partial V_j^{(1)}}{\partial x} = i\lambda V_j^{(1)} + i\Psi_j(x,0)V_j^{(2)},$$
$$\frac{\partial V_j^{(2)}}{\partial x} = -i\lambda V_j^{(2)} + i\Psi_j(x,0)V_j^{(1)}. \tag{43}$$

From a physical viewpoint the generation of the single quiescent soliton will occur with a smaller energy than the soliton pair.

Therefore, following the Ref. [13], we will define the number of the zeros of the Jost coefficients $a_j(\lambda)$ at $\lambda = 0$.

The formal solutions of Eq. (43) with $\lambda = 0$ are

$$V_1^{(1)}(x,0) = \exp(-iS_1(x))\left(C_1^{(1)}\int_{-\infty}^{x}\Psi_1(x',0)\exp\left(2iS_1(x')\right)dx' + C_1^{(2)}\right),$$
$$V_1^{(2)}(x,0) = -iC_1^{(1)}\exp(iS_1(x)) - V_1^{(1)}, \quad (44)$$

$$V_{2,3}^{(1)}(x,0) = \exp(-iS_{2,3}(x))\left(C_{2,3}^{(1)}\int_{0}^{x}\Psi_{2,3}(x',0)\exp\left(2iS_{2,3}(x')\right)dx' + C_{2,3}^{(2)}\right),$$
$$V_{2,3}^{(2)}(x,0) = -iC_{2,3}^{(1)}\exp(iS_{2,3}(x)) - V_{2,3}^{(1)}, \quad (45)$$

where

$$S_1(x) = \int_{-\infty}^{x}\Psi_1(x',0)dx',$$

and

$$S_{2,3}(x) = \int_{0}^{x}\Psi_{2,3}(x',0)dx'.$$

If one chooses $V_1^{(1)}(x,0) \to 0$ for $x \to -\infty$ and $V_{2,3}(x,0) \to 0$ for $x \to +0$, then $C_j^{(2)} = 0$, and we have

$$a_1(0) = \lim_{x\to -0} V_1^{(2)}(x,0) =$$
$$= -iC_1^{(1)}\left(\exp(iS_{01}) - i\exp(-iS_{01})\int_{-\infty}^{0}\Psi_1(x,0)\exp(2iS_1(x))dx\right)$$
$$= -iC_1^{(1)}\cos S_{01}, \quad (46)$$

$$a_{2,3}(0) = \lim_{x\to +\infty} V_{2,3}^{(2)}(x,0) =$$
$$= -iC_{2,3}^{(1)}\left(\exp(iS_{02,3}) - i\exp(-iS_{02,3})\int_{0}^{+\infty}\Psi_{2,3}(x,0)\exp(2iS_{2,3}(x))dx\right)$$
$$= -iC_{2,3}^{(1)}\cos S_{02,3}, \quad (47)$$

where

$$S_{0j} = \int_{e_j}\Psi_j(x,0)dx. \quad (48)$$

From Eqs. (46) and (47) for the soliton number we get

$$N = \left\langle \frac{3}{2} + \frac{S_{01}+S_{02}+S_{03}}{\pi}\right\rangle. \quad (49)$$

Noting that for the initial pulses guven by Eq. (41) for any x and with $\Psi_j(x,0) > 0$

$$S_{0j} \equiv \int_{e_j}\Psi_j(x,0)dx = \int_{e_j}|\psi_j(x,0)|dx = F_j. \quad (50)$$

we have from Eqs. (49) and (50)

$$N = \left\langle \frac{3}{2} + \frac{F_1+F_2+F_3}{\pi}\right\rangle. \quad (51)$$

Eq. (51) is the number of generated solitons in star graph. It is valid for arbitrary input pulse profile and number of bonds.

References

[1] Hasegawa A, Tappert F. Appl Phys Lett 1973;23:142.
[2] Mollenauer LF, Stolen RH, Gordon JP. Phys Rev Lett 1980;45:1095.
[3] Zakharov VE, Shabat AB. Sov Phys-JETP 1972;34:62.
[4] Bullough RK, Caudrey PJ. Solitons. Berlin: Springer; 1980.
[5] Scott AC, Chu FYF, McLaughlin DW. Proc IEEE 1973;61:1443.
[6] Satsuma J, Yajima N. Prog Theor Phys Suppl 1974;55:284.
[7] Hasegawa A, Kodama Y. Proc IEEE 1981;69:1145.
[8] Taylor JR. Optical solitons: theory and experiment. Cambridge, England: Cambridge University Press; 1992.
[9] Hasegawa A, Kodama Y. Solitons in optical communications. Oxford: Oxford University Press; 1995.
[10] Kivshar Y, Agrawal G. Optical solitons: from fibers to photonic crystals. Elsevier Science; 2003.
[11] Dauxois T, Peyrard M. Physics of solitons. Cambridge: Cambridge University Press; 2006.
[12] Burzlaff J. J Phys A 1988;21(561).
[13] Kivshar YS. J Phys A 1989;22(337).
[14] Gredeskul SA, Kivshar YS. Phys Rev Lett 1989;62(977).
[15] Fokas AS, Its AR. Phys Rev Lett 1992;68(3117).
[16] Panoiu N-C. Phys Rev A 1999;60(4).
[17] Nishizawa N, Okamura R, Goto T. Jpn J Appl Phys 1999;38(1).
[18] Panoiu N-C, Mel'nikov IV, Mihalache D, Etrich C, Lederer F. J Opt B 2002;4(R53).
[19] Skryabin DV, Yulin AV. Phys Rev E 2005;72(016619).
[20] Ganapathy R, Malomed BA, Porsezian K. Phys Lett A 2006;354(366).
[21] Carusotto I, Embriaco D, La Rocca GC. Phys Rev A 2002;65(4).
[22] Kartoshev YV. Opt Lett 2006;31(15).
[23] Chernikov SV, Taylor JR. Opt Lett 1994;19(8).
[24] Zhong X, Yao N, Sheng J, Cheng K. Opt Laser Tech 2018;99(1).
[25] Zhong X, Wu B, Cheng K. Optik (Stuttg) 2018;162(54).
[26] Sobirov Z, Matrasulov D, Sabirov K, Sawada S, Nakamura K. Phys Rev E 2010;81(066602).
[27] Sobirov Z, Matrasulov D, Sawada S, Nakamura K. Phys Rev E 2011;84(026609).
[28] Adami R, Cacciapuoti C, Finco D, Noja D. Rev Math Phys 2011;23(4).
[29] K Sabirov K, A Sobirov Z, Babajanov D, U Matrasulov D. Phys Lett A 2013;377(860).
[30] Noja D. Philos Trans R Soc A 2014;372(20130002).
[31] Caputo J-G, Dutykh D. Phys Rev E 2014;90(022912).
[32] Uecker H, Grieser D, Sobirov Z, Babajanov D, Matrasulov D. Phys Rev E 2015;91(023209).
[33] Noja D, Pelinovsky D, Shaikhova G. Nonlinearity 2015;28(2343).
[34] Adami R, Cacciapuoti C, Noja D. J Diff Eq 2016;260(7397).
[35] Sobirov Z, Babajanov D, Matrasulov D, Nakamura K, Uecker H. EPL 2016;115(50002).
[36] Adami R, Serra E, Tilli P. Commun Math Phys 2017;352(387).
[37] Kairzhan A, Pelinovsky DE. J Phys A 2018;51(95203).
[38] K Sabirov K, Rakhmanov S, Matrasulov D, Susanto H. Phys Lett A 2018;382(1092).
[39] Bolte J, Harrison J. J Phys A 2003;36(L433).
[40] K Sabirov K, Yusupov J, Jumanazarov D, Matrasulov D. Phys Lett A 2018;382(2856).
[41] Sabirov KK, Babajanov DB, Matrasulov DU, Kevrekidis PG. arXiv:1701.05707